Quaternary International
December 2011, Volume 246 Issue 1-2 Pages 203-212
https://doi.org/10.1016/j.quaint.2011.03.046
https://archimer.ifremer.fr/doc/00226/33774/

Sakurajima-Satsuma (Sz-S) and Noike-Yumugi (N-Ym) tephras: New tephrochronological marker beds for the last deglaciation, southern Kyushu, Japan

Moriwaki Hiroshi [1, *], Suzuki Takehiko [2], Murata Masanori [2], Ikehara Minoru [3], Machida Hiroshi, Lowe David J. [4]

[1] Kagoshima Univ, Fac Law Econ & Humanities, Kagoshima 8900065, Japan.
[2] Tokyo Metropolitan Univ, Dept Geog, Tokyo 158, Japan.
[3] Kochi Univ, Ctr Adv Marine Core Res, Kochi 780, Japan.
[4] Univ Waikato, Dept Earth & Ocean Sci, Hamilton 3240, New Zealand.

* Corresponding author : Hiroshi Moriwaki, email address : morih@leh.kagoshima-u.ac.jp

Abstract :

Two prominent tephras, Sakurajima-Satsuma (Sz-S) erupted from Sakurajima volcano and Noike-Yumugi (N-Ym) erupted from Kuchierabujima Island, provide new key marker beds for dating and synchronizing palaeoenvironmental and archaeological records in the last deglaciation in southern Japan. These tephras were identified on the basis of glass major-element compositions in two distal areas, a marine core (IMAGES MD982195) in the northern part of the East China Sea and on the central part of Tanegashima Island, and we related their stratigraphic positions to the marine oxygen isotope-based chronology. In MD982195, Sz-S, 0.8 cm in thickness at 9.12 m depth and N-Ym, 3 cm in thickness at 9.30 m depth, are both white, vitric, ash-grade tephras. On Tanegashima Island, Sz-S, 10 cm in thickness and N-Ym, 3 cm in thickness, are stratigraphically constrained by well-characterised marker tephras Kikai-Akahoya (7300 cal BP) and Aira-Tn (29,000 cal BP). Sz-S is rhyolitic and homogeneous on the basis of glass major-element compositions assayed by electron microprobe. Pumiceous glass shards predominant in distal Sz-S tephra indicate that it derived from pumice fall units that correspond to pumiceous and phreatomagmatic fine ash units constituting proximal Sz-S tephra. N-Ym is rhyolitic and glass major-element analyses reveal compositional diversity between units, suggesting that the lower and middle tephra units dispersed to the east, whereas the upper unit was dispersed north to northwest from the vent.

Stratigraphically, Sz-S occurs at around the start of the late-glacial reversal (cooling) in oxygen isotope records of MD982195, corresponding to the end of GI-1 and the start of GS-1 in the ice-core events of NGRIP (GICC05), consistent with a terrestrial age of similar to 12,800 cal BP. Based on the oxygen isotope stratigraphy, the tephra identified in the core as N-Ym at 9.30 m depth is close to the end of Greenland GI-1 and hence has an age of similar to 13,000 cal BP, but on Kuchierabujima Island it has an age based on C-14 assay of charcoal of c. 14,900 cal BR Although this age discrepancy (14.9 vs 13.0 cal ka) needs resolution, the occurrence in core MD982195 of N-Ym shows that it is more widespread than hitherto demonstrated. The widespread distributions and key stratigraphic positions for the two marker

tephras indicate that they are thus critical isochrons for precise correlation of palaeoenvironmental changes and prehistoric cultural events during the last deglaciation in southern Kyushu, and for relating such changes and events to the ice-core chronology via the marine oxygen isotope chronostratigraphy.

1. Introduction

The period from the last glacial to the present interglacial, known as the last deglaciation, is characterised by prominent rapid fluctuations in climate (Björck et al., 1998; Rasmussen et al., 2006, 2008). In order to examine the precise correlation and synchroneity or otherwise of such fluctuations in regional to global contexts, high-resolution ice-core, marine and terrestrial records have been developed through the INTIMATE project both in the North Atlantic region and in Australasia (Turney et al., 2006; Alloway et al., 2007; Hoek et al., 2008). A tephrochronological framework has been developed to help make precise correlations at regional scales during the last deglaciation, and widespread marker tephras, such as Vedde and Borrobol tephras (from Iceland), and the Rerewhakaaitu tephra (from New Zealand), have provided key isochrons for such correlations (Newnham et al., 2003; Lowe, D. et al., 2008, Lowe, J. et al., 2008).

In Japan, many records for marine and terrestrial palaeoenvironments in the last deglaciation have been obtained (e.g. Arai et al., 1981; Nakagawa et al., 2005; Hayashi et al., 2010). Although numerous tephra beds were deposited during the last deglaciation (Machida and Arai, 2003), relatively few have been identified that enable precise correlations of these marine, terrestrial, and ice-core records to be made. For example, the Ulleung-Oki tephra (10,700 cal BP, Kitagawa et al., 1995; Okuno et al., 2010) from Ulleung Island in Korea, is a useful time marker for correlating Holocene palaeoenvironmental records from the Japan Sea and terrestrial western Japan (Machida and Arai, 1983; Machida et al., 1984). As well, two very widespread marker tephras, Kikai-Akahoya tephra (K-Ah: 7,300 cal BP, Kitagawa et al., 1995) and Aira-Tn tephra (AT: 29,000 cal BP, Okuno, 2002) provide key benchmarks throughout Japan and adjacent seas.

In southern Kyushu, one of the most active volcanic regions in Japan, five major volcanic centres including large calderas and associated volcanoes, and the Tokara volcanic islands farther south, align south to north along the Ryukyu Island arc (Fig. 1) (Machida, 2010). More than 20 tephra beds have been recorded from those volcanoes between AT and K-Ah tephras (Moriwaki, 2010). Of these tephras, Sakurajima-Satsuma tephra (Sz-S) from Sakurajima volcano in the Aira volcanic centre (Kobayashi, 1986; Moriwaki, 1992; Machida and Arai, 2003) and Noike-Yumugi (N-Ym) from Kuchierabujima Island on the northern edge of the Tokara volcanic island chain (Geshi and Kobayashi, 2006; Moriwaki et al. 2009), are the most voluminous, suggesting that

they may be widespread in occurrence and thus potentially of great use for correlation purposes.

These two tephras were identified in a marine core, IMAGES MD98-2195 from the northern part of the East China Sea, and on the central part of Tanegashima Island at site T-1. These occurrences are the most distant yet identified of these eruptives (Fig. 1). Here, as part of the programme to develop a chronostratigraphic framework for the Kyushu-INTIMATE project (Integration of ice-core, marine and terrestrial records), the identification of these two tephras was examined, based on the chemical composition of glass shards and stratigraphic positions. The relationship of the marine record with the NGRIP ice-core chronology and hence implications for the chronology of the terrestrial palaeoenvironmental and archaeological records in southern Kyushu is discussed.

2. Distal occurrences of Sakurajima-Satsuma (Sz-S) and Noike-Yumugi (N-Ym) tephras

2.1 MD98-2195 core

MD98-2195 is located at 31 ° 38.33'N and 128 ° 56.63 ° E in the northern part of the East China Sea, 130 km west of Satsuma Peninsula, and in a water depth of 746 m. The core, currently stored at the Center for Advanced Marine Core Research, Kochi University, is 33.65 m in length, and dates back to 40,000 ^{14}C BP (Ijiri et al., 2005; Fig. 1). Palaeoenvironmental and marine oxygen isotope analyses were carried out on the core (Ijiri et al., 2005; Kawahata et al., 2006). K-Ah and AT tephras were identified at depths of 5.1–6.0 m and 21.8–22.9 m, respectively, and these, together with several ^{14}C dates, provide the age model for sediments of the last deglacial period (Ijiri et al., 2005). No tephras other than AT and K-Ah have been reported from this core.

MD98-2195 contains three thin, fine vitric ash beds (denoted A to C) visible within dark silty clay sediments between the AT and K-Ah tephra marker beds (Fig. 2). The uppermost tephra (MD98-2195-A) at 9.120-9.128 m depth comprises an 8-mm thick medium to fine-grained white ash layer that is lenticular in structure. This tephra is dominated by glass shards with minor amounts of primary pyroxene and feldspar. The glass shards contain abundant pumiceous, subordinate fibrous, and minor amounts of bubble-wall glass shards. The maximum grain size of the glass shards is ~ 0.3 mm. According to the age model of this core (Ijiri et al., 2005), the depth 9.120-9.128 m of tephra MD98-2195-A dates to 13,000 cal BP.

The middle tephra (MD98-2195-B), finer- grained than the uppermost ash, is pale grey in color and consists of a patchy ash zone 3 cm thick at 9.30-9.33 m depth. The tephra consists mostly of bubble wall glass shards. The age model of the core (Ijiri et al., 2005) yields 13,200 cal BP at 9.30-9.33 m, the depth of tephra MD98-2195-B.

The lowermost tephra (MD98-2195-C) is dark grey in color (very similar to the bracketing marine sediments) but is visibly distinguishable as a zone of notably coarse ash at 15.25-15.30 m depth. This tephra contains colorless and brown to pale brown glass shards with a maximum diameter of more than 0.4 mm. The colorless shards consist of pumiceous, fibrous, and platy bubble-walled morphologies in nearly equal proportions, whereas the brown to pale brown shards

are dominated by strongly vesicular pumiceous textures and markedly contain non-vesicular chunky textures. The age model of the core (Ijiri et al., 2005) yields 19,800 cal BP at 15.25-15.30 m, the depth of tephra MD98-2195-C.

2.2 Tanegashima Island

Tanegashima Island lies ~30 km south of Osumi Peninsula, southern Kyushu Island. At location T-1 (30 ° 38'36.35" N, 130 ° 59'24.43"E) in the central part of the island (Fig. 1), a well-preserved ~3-m-high sequence of late Pleistocene tephra beds includes the K-Ah and AT tephras. Three tephra beds, T-1-1, T-1-2, and T-1-3 (from upper to lower) occur between them (Fig. 2). The uppermost tephra (T-1-1) is a fine-grained vitric ash bed, 10 cm thick and orange in color. The middle tephra (T-1-2) is 3 cm thick and coarser-grained than T-1-1. It contains dominantly grey and orange pumice clasts, which reveal compositional diversity (see analyses below). The lowermost tephra (T-1-3), dark grey in color, is a fine scoriaceous ash bed.

2.3 Possible correlatives for the newly-discovered distal tephras

Tephrostratigraphic frameworks spanning the last deglaciation have been erected for each volcanic centre in southern Kyushu based on proximal stratigraphies (Okuno, 2002; Machida and Arai, 2003, Moriwaki, 2010). Of these proximal tephras, the most likely correlatives of tephras MD98-2195-A and MD98-2195-B, and of tephras T-1-1 and T-1-2 – in terms of stratigraphy and volume – are Sakurajima-Satsuma tephra (Sz-S) erupted from Sakurajima volcano in the Aira volcanic centre (Kobayashi, 1986; Moriwaki, 1992) and Noike-Yumugi tephra (N-Ym) erupted from Kuchierabujima Island situated at the northern tip of the Tokara volcanic chain (which includes six major active volcanic islands) (Fig. 1) (Geshi and Kobayashi, 2006; Moriwaki et al., 2009).

Sz-S is the most voluminous of ~ 17 tephras erupted from the Sakurajima volcano in the past ~26,000 cal yrs (Kobayashi, 1986; Moriwaki, 1994; Moriwaki, 2010). It is estimated to be ~11 km^3 in bulk volume (Kobayashi and Tameike, 2002). It consists of more than 10 members, which are mostly pumice fall beds together with a pair of phreatomagmatic fine-grained ash-fall beds and a base surge deposit (Moriwaki, 1992) (Figs. 1 and 3). Sz-S occurs not only in the Osumi Peninsula, on which most tephras prevail eastward from source vents because of prevailing westerlies, but also notably on the Satsuma Peninsula westward from Sakurajima volcano, collectively forming a circular distribution pattern (Kobayashi, 1986; Moriwaki, 1992).

Regarding the age of Sz-S, 10,500 ^{14}C BP was given on the basis of several dates for charcoal in Sz-S measured by the beta counting (liquid scintillation) method (Machida and Arai, 1992). Okuno et al. (1997) estimated the age of Sz-S as 11,500 ^{14}C BP on the basis of dates obtained by the AMS dating method on humic soils immediately below Sz-S. Okuno (2002) determined a calibrated age of 12,800 cal BP for Sz-S on the basis of a revised ^{14}C age of 11,000 ^{14}C BP. This last age is the only calibrated age obtained thus far for the Sz-S tephra, hence 12,800 cal BP is

used for the terrestrial age of Sz-S in this paper. Although Okuno et al. (1997) considered the gap of 1000 years between 10,500 and 11,500 ^{14}C BP probably to be due to the different methods of assay (i.e., beta counting *vs.* AMS), it may alternatively be attributable to differences in sample types and their stratigraphic juxtapositions i.e., assay of humic material in soils below Sz-S *vs.* charcoal within Sz-S. The dating of Sz-S tephra deposits needs further examination to improve the precision of their eruptive age.

N-Ym was erupted from the Noike vent in the Kuchierabujima volcanic complex, located in the central part of Kuchierabujima Island (Geshi and Kobayashi, 2006) (Figs. 1 and 3). The tephrostratigraphic position of N-Ym is constrained by K-Ah (above) and AT (below) (Geshi and Kobayashi, 2006; Moriwaki et al., 2009). N-Ym consists of pumice fall deposits underlying a thin pyroclastic flow deposit and contains banded pumices and scoriae showing compositional diversity. These fall and flow units constitute a single tephra formation without a time gap between the units. The maximum thickness for the entire deposit exceeds 5 m around the vent, and it is the most voluminous of the tephras erupted from the Tokara volcanic chain during the last deglaciation (Geshi and Kobayashi, 2006; Moriwaki et al., 2009). The N-Ym eruption probably attained a VEI of 6, judging from the widespread occurrences revealed in this paper. The isopachs on Kuchierabujima Island show the main distributions to have been north and east of the vent.

N-Ym is dated between 15,560 and 14,280 cal BP (median ~14,900 cal BP) on the basis of a ^{14}C age (12,600±70 ^{14}C BP) obtained on charcoal in the pumice fall deposit (Moriwaki et al., 2009), and between 14,900 and 14,150 cal BP (median ~14,500 cal BP) on the basis of a ^{14}C age (12,440±60 ^{14}C BP) on charcoal in the pyroclastic flow deposit on the island (Geshi and Kobayashi, 2006). Kobayashi et al. (2002) obtained an age of 12,435±50 ^{14}C yr BP on charcoal in the pumice fall deposit. Although those ages show relatively good agreement, their precision is insufficient for examining the high-resolution chronology required for palaeoenvironmental reconstructions. It is necessary both to collect more high-precision dates on optimum dating material for N-Ym and Sz-S, and to employ a Bayesian statistical approach to calibrate sequences of ages using flexible age-sediment modeling. Such modelling provides enhanced and more precise chronologies expressed as probabilities (e.g., Wohlfarth et al., 2006; Blockley et al., 2008; Lowe, D. et al., 2008).

3. Characterization and identification

Glass chemical compositions are typically used to identify distal tephras (Lowe, 2011). Major-element compositions of the glass shards were obtained for the three distal tephras in core MD98-2195 and at T-1 on Tanegashima Island using electron microprobes of Kagoshima University, Tokyo Metropolitan University, and the University of Toronto. Conditions of analysis are noted in Table 1. Any small differences in composition relating to the deployment of these different instruments were checked using glass shards of AT tephra (Table 1), which is very homogeneous with respect to major elements and thus provides a useful in-house standard for

checking analytical reproducibility (Machida and Arai, 2003). Analyses of AT glass shards showed that the electron microprobe of Tokyo Metropolitan University underestimated both CaO (by 0.43 wt%, mean value) and Na_2O (by 0.56 wt%), and overestimated K_2O (by 0.28 wt%) in comparison with analyses obtained using the electron microprobes at the University of Toronto and Kagoshima University. Other oxides, however, are essentially concordant between the three instruments (Table 1). Therefore, correction factors were applied for these three oxides for the glass major-element compositions of tephras MD98-2195-A, -B and -C that were analysed at Tokyo Metropolitan University (Figs. 4 and 5). The major-element compositions of glass obtained from samples of the Sz-S and N-Ym tephras at proximal reference localities are given in Table 2. Analyses of glass shards from samples of the distal tephras MD98-2195-A, -B and- C (analysed at Tokyo Metropolitan University), and from T-1-1 and T-1-2 on Tanegashima Island (analysed at Kagoshima University), are shown in Table 3. All data are normalized to a 100%-water free basis.

3.1 Sakurajima-Satsuma (Sz-S) tephra

The average major-element compositions (Table 2) and oxide bivariate plots using the major elements of individual glass shards (Fig. 4) show that the major-element compositions analysed for several members of Sz-S at reference sites on the Osumi and Satsuma peninsulas are very similar, demonstrating they are derived from homogeneous magma: the major elements of the all members of Satsuma and Osumi peninsulas lie within 74-76 wt% for SiO_2, 13-14 wt% for Al_2O_3, 0.2-0.6 wt% for TiO_2, 1.6-2.2 wt% for FeO_t, 1.5-2.5 wt% for CaO, and 2.7-3.2 wt% for K_2O. Thus it is not possible to distinguish between the members on Osumi and Satsuma peninsulas on the basis of the major element compositions. The Sz-S glasses are classified as high silica-rhyolite (Le Bas et al., 1986).

Fig. 4 and Table 3 show that the uppermost tephra bed, MD98-2195-A in the northern part of the East China Sea, and tephra T-1-1 on Tanegashima Island, are similar in composition to the proximal Sz-S tephras, indicating that these two distal tephra beds are likely correlatives of Sz-S tephra. Although it is impossible to correlate the distal tephras to specific members of Sz-S using glass-shard major elements alone (because glasses of the Sz-S members are all identical compositionally with regard to major elements), the predominance of pumiceous glass shards in the distal tephra bed MD98-2195-A suggests that it is derived from plinian fall-out pumice members (Fig. 3).

3.2 Noike-Yumugi (N-Ym) tephra

Proximal N-Ym is classed as a rhyolite (Table 2) (Le Bas et al., 1986). However, the major-element compositions of N-Ym are diverse, not only stratigraphically but also within the same member as evidenced by the wide values for standard deviation (Moriwaki, et al., 2009: Table 2, Fig. 5). The values in the six diagrams (Fig. 5) show a wide dispersion and distinctively bimodal composition (Moriwaki et al., 2009). Upper, middle, and lower units are classed (using

non-normalised compositions) as a rhyolite, a dacite and a rhyodacite, respectively (Le Bas et al., 1986). For example, the upper unit (KU5) of N-Ym shows bimodal composition in the SiO_2-Al_2O_3 diagram: one mode with high SiO_2 (77-79 wt%) and low Al_2O_3(11.9-12.5 wt %), and the other, low SiO_2 (74 wt%) and high Al_2O_3(13 wt%), and one with high TiO_2 (0.5-0.7 wt%) and high FeOt (2.4-2.5 wt%), and the other, low TiO_2 (0.14 – 0.4 wt%) in the FeO_t-TiO_2 diagram. Similarly, the middle unit (KU4) has a wide range in composition with low SiO_2(72-75 wt %) and high Al_2O_3 (12.8-14.2 wt%) in the SiO_2- Al_2O_3 diagram, and high TiO_2 (0.5-0.8 wt%) and high FeOt (2.7-3.8 wt%) in the FeO_t-TiO_2 diagram. The lower unit (KU2) shows a narrow range in composition with low SiO_2 (74-76 wt%) and high Al_2O_3 (12.7-13.1 wt%) in the SiO_2- Al_2O_3 diagram, and wide range for TiO_2 but narrow for FeOt in composition with relatively high TiO_2 (0.3-0.7 wt %) and relatively high FeOt (2.3-2.7 wt%)(Fig. 5). Such heterogeneity is consistent with the occurrences of banded pumices and scoriae in N-Ym tephra bed at the proximal reference locations described earlier.

The distal tephras, T-1-2 on Tanegashima and tephras MD98-2195-B and MD98-2195-C in the East China Sea, are classified as high-silica rhyolites based on glass major-element compositions (Table 3) (LeBas et al., 1986). Significantly lower CaO and higher K_2O contents for tephras MD98-2195-B and MD98-2195-C, relative to those of tephra T-1-2, are possibly due to the differences resulting from the different electron microprobes used, as evidenced by the AT glass chemical compositions (analyses in Table 3 are reported uncorrected). The wide compositional range present in samples from tephras T-1-2, MD98-2195-B, and MD98-2195-C, combined with the limited number of analyses obtainable, make it difficult to directly compare the resulting average composition with the proximal composition of N-Ym tephra bed. This wide compositional range is reflected in the large standard deviations obtained for these samples. The proximal pumice fall deposits of N-Ym are similarly diverse. In these circumstances, the distribution of individual glass shards analyses can be used to characterize tephras MD98-2195-B, MD98-2195-C, and T-1-2, and to explore potential correlations amongst themselves and the N-Ym tephra bed (Fig. 5).

The values in the six biplots (Fig. 5) show a wide dispersion and distinctively bimodal composition in every ash bed, which mimic those of the proximal N-Ym pumice fall deposits on Kuchierabujima Island (Moriwaki et al., 2009) and collectively reveal similar patterns in both distal and proximal tephras. In more detail, tephra T-1-2 on Tanegashima Island is compositionally similar to the middle and lower units of the proximal N-Ym tephra bed on Kuchierabujima Island, as exemplified in the SiO_2- Al_2O_3 diagram with contents of low SiO_2 (75-76 wt%) and high Al_2O_3 (12.7-13.4 wt%) , and, in the FeO_t-TiO_2 diagram, high TiO_2 (0.29-0.59 wt%) and high FeOt (2.3-2.5 wt%) . Tephra T-1-2 is likely correlated to these units, thus showing that lower and middle units of N-Ym fall-out pumice were dispersed eastward from the vent.

Tephras MD98-2195-B and MD98-2195-C, although stratigraphically separated by ~ 6 m (Fig. 2), are both similar compositionally to the upper unit of N-Ym. In particular, glass analyses (of B

and C) match one of the bimodal populations of N-Ym as exemplified in the SiO_2-Al_2O_3 and FeO_t-TiO_2 diagrams (Fig. 5), which shows prominently high SiO_2 (77-79 wt%)and low Al_2O_3 (11.7-12.3 wt%) in the first population, and low SiO_2 (72-76 wt%%) and high Al_2O_3(13.4-12.6 wt%) in the second population (although the values in the second population are rather dispersed), and low FeO_t (0.9-1.8 wt%) and low TiO2 (0.1-0.5 wt%) in the first population and high FeO_t (2.2-3.1 wt%) and high TiO_2 (0.4-0.7 wt%) in the second population. Considering the stratigraphic juxtapositions of the two tephra beds, tephra MD98-2195-B is likely correlated with the upper unit of the N-Ym tephra as at proximal locations, although it is difficult to show that it is distinctly different from tephra MD98-2195-C by the use of major element compositions alone.

Tephra MD98-2195-C, aged ~19,800 cal BP on the basis of the marine oxygen isotope stratigraphy (Fig. 6), is a different tephra bed derived probably from an eruption on Kuchierabujima Island. The correlation of tephra MD98-2195-B with the upper units of N-Ym fall-out tephra indicates that these eruptives were dispersed north to northwestward from Kuchierabujima Island.

Thus, tephra deposits such as tephra MD98-2195-B, which is heterogeneous in composition, nevertheless have the potential to be correlated although the analytical data require careful examination (Shane et al., 2003, 2008; Lowe, D. et al., 2008).

4. Implications

4.1 Stratigraphic positions with respect to marine oxygen isotope record and age relationships

The Sz-S and N-Ym tephras, correlated here with tephras MD98-2195-A and MD98-2195-B, respectively, can be related stratigraphically to changes evident in the marine oxygen isotope record for the last deglaciation in the same core (Fig. 6; Ijiri et al., 2005).

Tephra Sz-S occurs at around the start of the late-glacial reversal (cooling) in the oxygen isotope records of MD98-2195 (Ijiri et al., 2005) and an approximate peak in abundance of arboreal pollen (Kawahata and Oshima, 2004), which in turn corresponds to the end of GI-1 and the start of GS-1 in the ice-core events of NGRIP (GICC05) (Lowe, J. et al., 2008). The age model of MD98-2195 core (Ijiri et al. 2005) generates an age for tephra Sz-S as ~ 13,000 cal BP, as noted earlier. Given that the transition peaks of the isotopic records of MD98-2195 and NGRIP (GICC05) are simultaneous, the age of Sz-S is estimated at ~ 13,000-12,800 cal BP according to the age of the peak in NGRIP/GICC05, which nearly corresponds to that of the age model of MD98-2195.

The age of tephra Sz-S, estimated on land at 12,800 cal BP (Okuno, 2002), nearly coincides with that based on ^{14}C ages recorded in the marine core (Ijiri et al., 2005), and matches in age the approximate boundary between the events GI-1a and GS-1 in the NGRIP/GICC05 isotopic records (Lowe, J. et al., 2008; Rasmussen et al., 2008). Thus, the equivalent stratigraphic position of tephra Sz-S in the NGRIP ice core records nearly corresponds to both the ^{14}C age of Sz-S obtained from terrestrial records and that derived from the marine oxygen isotope record of MD98-2195. At a higher resolution scale, there are slight differences in age between the records,

mainly relating to the position of the boundary of events GS-1 and GI-1, or GI-1a. Although such a difference may in theory be due to a climatic change being recorded in the East China Sea before such a change was recorded in Greenland, it is more likely a result of the relative imprecision of the ^{14}C ages thus far obtained on Sz-S. Obtaining a more precise age for Sz-S will allow the age models for the marine record to be improved.

In contrast, based on oxygen isotope stratigraphy, tephra MD98-2195-B identified in the core as N-Ym at 9.30-9.33 m depth occurs near the end of Greenland GI-1, which has an age of ~13,200 cal BP using the age model of the marine core (Ijiri et al., 2005; Lowe, J. et al., 2008) (Fig. 6). Given that the transition peaks of the isotopic records of MD98-2195 and NGRIP (GICC05) are simultaneous, the age of N-Ym is estimated at 13000–13,200 cal BP, which nearly corresponds to that of the age model of MD98-2195 (Ijiri et al., 2005). However, the age of N-Ym on land is estimated at 14,900–14500 cal BP. Although this age discrepancy (14.9-14.5 *vs.* 13.2 cal ka) needs resolution, the occurrence in core MD98-2195 of N-Ym, assuming the correlation is sound, shows that it is more widespread than hitherto demonstrated.

These newly identified occurrences of Sz-S and N-Ym tephras in the marine core provide potential for examining the relationship between regional palaeoenvironments including climatic changes of southern Kyushu and how such changes relate to the ice-core chronostratigraphy. Thus tephras Sz-S and N-Ym supplement previously well-known marker tephras K-Ah and AT and together provide an enhanced tephrochronological framework to enable marine, ice and terrestrial records to be linked, as occurs for records of the last deglaciation in the North Atlantic and elsewhere (Lowe, J. et al., 2001, 2008; Lowe, D. et al., 2008).

4.2 Distributions of Sz-S and N-Ym tephras

Core MD98-2195 and the central part of Tanegashima Island lie c. 190 km west and c. 120 km south of the Sz-S source vent, Sakurajima volcano, respectively. Similarly, MD98-2195 and the central part of Tanegashima Island lie c.180 km northwest and c. 80 km east of the N-Ym source vent, Noike vent on Kuchierabujima Island, respectively. Tephras Sz-S and N-Ym thus were distributed in various directions from the source volcanoes and their areas of distribution amount to more than 80,000 km^2 and 30,000 km^2, respectively (Fig. 7). The VEIs for both are likely to be 6. In particular, tephra Sz-S extensively occurs not only over all of terrestrial southern Kyushu, but also in the northern part of the East China Sea and Pacific Ocean off southern Kyushu. Further investigations on cryptotephras over more distant areas will enable the distribution of both tephras to be mapped even further afield (e.g. Lowe, 2011).

4.3 Palaeoenvironmental changes and cultural events

Tephra Sz-S has been widely recognised on land in southern Kyushu and utilised as a prominent time-parallel marker for precisely correlating and dating palaeoenvironmental and human records (Moriwaki et al., 2010).

Kameyama et al. (2005) indicated that Aira caldera was submerged under seawater between

about 11,700 and 11,000 ^{14}C BP. Such submergence was likely a consequence of the collapse of the southern caldera wall as a result of the Sz-S eruption. On the other hand, tephra Sz-S occurs in the coastal-lowland deposits of the last deglaciation in southern Kyushu, and the stratigraphic relation of tephra Sz-S to the depositional history and sea-level change shows that the relative sea-level at the time of Sz-S lies ~50 m below present sea-level on the coastal lowland and that the evidence of initial marine invasion of the coastal lowland lies ~4 m below Sz-S (Moriwaki et al., 2005). These findings show therefore that the marine invasion of Aira caldera within Kagoshima Bay occurred before the Sz-S eruption (Moriwaki et al., 2005), indicating that the inundation was not due to the collapse of caldera wall at the time of the Sz-S eruption. The stratigraphic position of tephra Sz-S, based on correlation of the marine oxygen isotope record of MD98-2195 to that of NGRIP (GICC05), demonstrates that the transgression likely reflects rapid sea-level rise caused by melt-water pulse Ia (Fairbanks, 1989; Bard et al., 1996). The occurrence of the 'wet' phreatomagmatic eruptions of Sz-S suggests that these eruptions involved seawater interaction with magma and thus took place when sea-level was ~50 m below the present level (Moriwaki, 1994).

In terms of human culture, tephra Sz-S is a critical isochron for marking the stratigraphic position of the end of the microblade culture, the beginning of housing settlement, and the beginning of ceramic culture in southern Kyushu (Moriwaki et al., 2010), which were prominent changes for prehistoric archaeology of Japan.

5. Conclusions

Key marker tephras of the last deglaciation, the Sakurajima-Satsuma (Sz-S) tephra from Sakurajima volcano and the Noike-Yumugi (N-Ym) tephra from Kuchierabujima Island, were identified in a marine core (IMAGES MD98-2195) in northern part of the East China Sea and on central Tanegashima Island on the basis of glass-chemical composition and stratigraphic associations. Sz-S tephra is rhyolitic and homogeneous in glass major-element composition. N-Ym is also rhyolitic, but diverse in composition both stratigraphically as well as within individual clasts. Stratigraphically, tephra Sz-S, dated at 12,800 cal BP, occurs at around the start of the late-glacial reversal (cooling) in oxygen isotope records of MD98-2195 (Ijiri et al., 2005), which corresponds to the end of GI-1 and the start of GS-1 in the ice-core events of NGRIP (GICC05) (Lowe, J. et al., 2008). Tephra N-Ym, erupted before tephra Sz-S, marks the end of GI-1 as determined for MD98-2195 and thus has an age of ~13,000 cal BP based on the oxygen isotope stratigraphy in MD98-2195. However, an age of between 14,500 and 14,900 cal BP has been obtained for proximal N-Ym tephra, and so there is a discrepancy with these records. Either the identification of MD98-2195-B is incorrect or the ages are not correct, or both. Alternatively, part of core MD98-2195 may be missing (as can occur, e.g., see Carter et al., 1995). Tephra MD98-2195-C, close to ~20,000 cal BP on the basis of its position in MD98-2195 (Fig. 6), currently remains uncorrelated.

The occurrences of Sz-S and N-Ym tephras in core MD98-2195 and on Tanegashima Island

reveal that those tephras are more widespread than previously demonstrated. The distal ash of Sz-S is likely sourced from the fall-out pumice units of proximal deposits. Glass chemical compositions of stratigraphically distinguishable units of N-Ym tephra suggest that the lower and middle units of N-Ym fall beds were dispersed to the east whereas the upper beds of N-Ym were dispersed to the north to northwest.

The distributions and stratigraphic positions in the oxygen isotope records of marine core MD98-2195 mean that these two newly identified tephras, Sz-S and N-Ym, together with AT and K-Ah, can help refine the chronology of the terrestrial palaeoenvironmental and archaeological records in southern Kyushu. These identifications form part of the programme to develop a more detailed chronostratigraphic framework for the Kyushu-INTIMATE project targeted at the past 30,000 years.

Acknowledgments

We are grateful to John Westgate (University of Toronto) for his suggestion to undertake glass-shard major element analyses of the tephras as reported here, and to Tadamichi Oba for his suggestion to obtain tephra samples. We thank Tetsuo Kobayashi for providing information on the ages of terrestrial tephras. We are also very grateful for helpful comments on the paper by anonymous referees. A fellowship from the Japan Society for the Promotion of Science permitted David J. Lowe to visit Japan in May, 2010, and that support is gratefully acknowledged. Part of the research was supported by a grant-in-aid for the Japan Society for the Promotion of Science, No. 21501001. This paper is an output associated with the INTREPID project (INQUA-0907), "Enhancing tephrochronology as a global research tool through improved fingerprinting and correlation techniques and uncertainty modeling", which is supported by the International Union for Quaternary Research.

References

Alloway, B.V., Lowe, D.J., Barrell, D.J.A., Newnham, R.M.., Almond, P.C., Augustinus, P.C., Bertler, N.A., Carter, L., Litchfield, N.J., McGlone, M.S., Shulmeister, J., Vandergoes, M.J., Williams, P.W., NZ-INTIMATE members, 2007. Towards a climate event stratigraphy for New Zealand over the past 30,000 years (NZ-INTIMATE project). Journal of Quaternary Science 22, 9-35.

Arai, F., Oba, T., Kitazato, Y., Horibe, Y., Machida, H., 1981. Late Quaternary tephrochronology and palaeoceanography of the sediments of the Japan Sea. The Quaternary Research of Japan, 20, 209-230. (In Japanese with English abstract.)

Bard, E., Hamelin, B., Arnold, M., Montaggioni, L., Cabioch, G., Faure, G., Rougerie, F., 1996. Deglacial sea-level record from Tahiti corals and the timing of global meltwater discharge. Nature 382, 241-244.

Björck, S., Walker, M.J.C., Cwynar, L.C., Johnsen, S., Knudsen, K.L., Lowe, J.J., Wohlfarth, B., INTIMATE members, 1998. An event stratigraphy for the last termination in the North

Atlantic region based on the Greenland ice-core record: a proposal by the INTIMATE group. Journal of Quaternary Science 13, 283–292.

Blockley, S.P.E., Bronk Ramsey, C., Lane, C.S., Lotter, A.F., 2008. Improved age modelling approaches as exemplified by the revised chronology for the central European varved lake Soppensee. Quaternary Science Reviews 27, 61-71.

Carter, L., Nelson, C.., Neil, H.L., Froggatt, P.C., 1995. Correlation, dispersal, and preservation of the Kawakawa Tephra and other late Quaternary tephra layers in the southwest Pacific Ocean. New Zealand Journal of Geology and Geophysics 38, 29-46.

Fairbanks, R.G., 1989. Glacio-eustatic record 0–16,000 years before present: influence of glacial melting rates on Younger Dryas event and deep ocean circulation. Nature 34, 637–642.

Geshi, N., Kobayashi, T., 2006. Volcanic activities of Kuchinoerabujima Volcano within the last 30,000 years. Bulletin of the Volcanological Society of Japan, 51, 1-20. (In Japanese with English abstract.)

Hayashi, R., Takahara, H., Hayashida, A., Takemura, K., 2010. Millennial-scale vegetation changes during the last 40,000 yr based on a pollen record from Lake Biwa, Japan. Quaternary Research 74, 91-99.

Hoek, W.Z., Yu, Z.C., Lowe, J.J., 2008. INTegration of Ice-core, MArine and TErrestrial records (INTIMATE): refining the record for the Last Glacial-Interglacial Transition. Quaternary Science reviews 27, 1-5.

Ijiri, A. Wan, L., Oba, T., Kawahata, H., Huang, C- Y., Huan, C- Y., 2005. Paleoenvironmental changes in the northern area of the East China Sea during the past 42,000 years. Palaeogeography, Palaeoclimatology, Palaeoecology 219, 239-261.

Kameyama, S., Shimoyama, S., Miyabe, S., Miyata, Y., Sugiyama, T., Iwano, H., Danhara, T., Endo, K., Matsukuma, A., 2005. Stratigraphy and ages of Aira caldera deposits in Shinjima (Moeshima), Kagoshima prefecture, west Japan. The Quaternary Research of Japan 44 , 15-19. (In Japanese with English abstract.)

Kawahata, H. and Oshima, H., 2004. Vegetation and environmental record in the northern East China Sea during the late Pleistocene. Global and Planetary Change 41, 251-273.

Kawahata, H., Nohara, M., Aoki, K., Minoshima, K., Gupta, L., 2006. Biogenic and abiogenic sedimentation in the northern East China Sea in response to sea-level change during the late Pleistocene. Global and Planetary Change 53, 108-121.

Kitagawa, H., Fukusawa, H., Nakamur, T., Okamura, M., Takemura, K., Hayashida, A., Yasuda, Y., 1995. AMS ^{14}C dating of varved sediments from Lake Suigetsu, central Japan and atmospheric ^{14}C change during the late Pleistocene. Radiocarbon 37, 371–378.

Kobayashi, T., 1986. Volcanic history and pyroclastic flows of Sakurajima Volcano. In: Aramaki, S. (Ed), Characteristics of dry high concentration flows (pyroclastic flows) associated with volcanic eruption and their disasters, pp.137-163. (In Japanese.)

Kobayashi, T., Okuno, M., Nakamura, T., 2002. Eruption history of Kuchierabu volcano. Sakurajima Volcano Research Center, Disaster Prevention Research Institute Kyoto

University (ed.) "Satsuma-Iojima kazan, Kuchierabujima kazan no shuchu sogo kansoku" 169-178. (In Japanese.)

Kobayashi, T., Tameike, T., 2002. History of eruptions and volcanic damage from Sakurajima Volcano, southern Kyushu, Japan. The Quaternary Research of Japan 41, 269-278. (In Japanese with English abstract.)

LeBas, M.J., LeMaitre, R.W., Streckeisen, A., Zanettin, B., 1986. A chemical classification of volcanic rocks based on the total alkali-silica diagram. Journal of Petrology 27, 745-750.

Lowe, D.J., 2011. Tephrochronology and its application: a review. Quaternary Geochronology 6, 107-153.

Lowe, D.J., Shane, P.A.R., Alloway, B.V., Newnham, R.M., 2008. Fingerprints and age models for widespread New Zealand tephra marker beds erupted since 30,000 years ago: a framework for NZ-INTIMATE. Quaternary Science Reviews 27, 95-126.

Lowe, J.J., Hoek, W.Z., INTIMATE group, 2001. Inter-regional correlation of palaeoclimatic records for the Last Glacial-Interglacial Transition: a protocol for improved precision recommended by the INTIMATE project group. Quaternary Science Reviews 20, 1175-1187.

Lowe, J.J., Rasmussen, S.O., Björck, S., Hoek, W.Z. Steffensen, J.P. Walker, M.J.C., Yu, Z.C., INTIMATE group, 2008. Synchronisation of palaeoenvironmental events in the North Atlantic region during the Last Termination: a revised protocol recommended by the INTIMATE group. Quaternary Science Reviews 27, 6-17.

Machida, H., 2010. Outline of tectonic setting and explosive volcanism of southern Kyushu. In: Moriwaki, H., Lowe, D. J. (Eds), Intra-conference Field Trip Guides. INTAV International Field Conference on Tephrochronology, Volcanism, and Human Activity, Kirishima City, Kyushu, Japan, 9-17 May, 2010, pp.11-35.

Machida, H., Arai, F., 1983. Extensive ash falls in and around the Sea of Japan from large late Quaternary eruptions. Journal of Volcanology and Geothermal Research 18, 151-164.

Machida, H. and Arai, F., 1992. Atlas of Tephra in and Around Japan. University of Tokyo Press, 276pp. (In Japanese.)

Machida, H. and Arai, F., 2003. Atlas of Tephra in and Around Japan (Revised Ed.). University of Tokyo Press, 336pp. (In Japanese.)

Machida, H., Arai, F., Lee, B-S., Moriwaki, H., Furuta, T., 1984. Late Quaternary tephras in Ulreung-do Island, Korea. Journal of Geography of Japan 93, 1-14. (In Japanese with English abstract.)

Machida,. H., Arai, F., Sugihara, S., Oda, S., Endo, K., 1984. Tephra and Japan Archaeology - Tephra Catalogue related to Archaeological research - . Watanabe, N. (ed.) " General Report on Conservation Science related to Cultural Properties and Human and Natural Science". 865-928. (Tefura to Nihon Kokogaku - Kokogaku Kenkyu to kankeisuru Tefura no Katarogu -. Watanabe N., (ed.) Kobunkazai ni kansuru Hozonkagaku to Jinbun-Shizen Kagaku - Sokatsu Hokokusho - , 865-928. (In Japanese)

Moriwaki, H., 1992. Late Quaternary phreatomagmatic tephra layers and their relation to

paleo-sea levels in the area of Aira caldera, southern Kyushu, Japan. Quaternary International 13/14, 195-200.

Moriwaki, H., 1994. Palaeoenvironmental study on late Quaternary fine ash beds around Kagoshima Bay. Reports for Grants-in-Aid for Scientific Research (no. 04680248) from Ministry of Education, 68pp. (In Japanese.)

Moriwaki, H., 2010. Late Pleistocene and Holocene tephras in southern Kyushu. In: Moriwaki, H., Lowe, D. J. (eds), Intra-conference Field Trip Guides. INTAV International Field Conference on Tephrochronology, Volcanism, and Human Activity, Kirishima City, Kyushu, Japan, 9-17 May, 2010, pp.44-53.

Moriwaki, H., Nagasako, T., Arai, F., 2009. Late Pleistocene and Holocene tephras in the Tokara Islands, southern Japan. The Quaternary Research of Japan 48, 271-287. (In Japanese with English abstract.)

Moriwaki, H., Nakamura, N., Sangawa, T., 2010. Tephras and archaeology in southern Kyushu. In: Moriwaki, H., Lowe, D. J. (eds), Intra-conference Field Trip Guides. INTAV International Field Conference on Tephrochronology, Volcanism, and Human Activity, Kirishima City, Kyushu, Japan, 9-17 May, 2010, pp.71-75.

Moriwaki, H., Ohira, A., Matsushima, Y., Oki, K., 2005. Tephrochronology of Holocene deposits and palaeoenvironmental change in Kokubu lowland, southern Kyushu, Japan. Abstract for the Congress of Japan Association for Quaternary Research, No. 35, 131-132. (In Japanese.)

Nakagawa, T., Kitagawa, H., Yasuda, Y., Tarasov, P.E., Gotanda, K., Sawai, Y., 2005. Pollen/event stratigraphy of the varved sediment of Lake Suigetsu, central Japan from 15,701 to 10,217 SG vyr BP (Suigetsu varve years before present): description, interpretation, and correlation with other regions. Quaternary Science Reviews 24, 1691–1701.

Newnham, R.M., Eden, D.N., Lowe, D.J., Hendy, C.H., 2003. Rerewhakaaitu Tephra, a land-sea marker for the Last Termination in New Zealand, with implications for global climate change. Quaternary Science Reviews 22, 289-308.

Okuno, M., 2002. Chronology of tephra layers in southern Kyushu, SW Japan, for the last 30,000 years. The Quaternary Research of Japan 41, 225-236. (In Japanese with English abstract.)

Okuno, M., Nakamura, T., Moriwaki, H., Kobayashi, T., 1997. AMS radiocarbon dating of the Sakurajima tephra group, southern Kyushu, Japan. Nuclear Instruments and Methods in Physics Research B 123, 470-474.

Okuno, M., Shiihara, M., Torii, M., Nakamura, T., Kim, K. Domitsu, H., Moriwaki, H., Oda, M., 2010. AMS radiocarbon dating of the Holocene tephra layers on Ulleung Island, South Korea. Radiocarbon 52, 1465-1470.

Rasmussen, S.O., Andersen, K.K., Svensson, A.M., Steffensen, J.P.,Vinther, B., Clausen, H.B., Siggaard-Andersen, M.-L., Johnsen, S.J., Larsen, L.B., Dahl-Jensen, D., Bigler, M., Röthlisberger, R., Fischer, H., Goto-Azuma, K., Hansson, M., Ruth, U., 2006. A new Greenland ice core chronology for the last glacial termination. Journal of Geophysical Research 111, D06102.

Rasmussen, S.O., Seierstad, I.K., Anderson, K.K., Bigler, M., Dahl-Jensen, D., Johnsen, S.J., 2008. Synchronization of the NGRIP, GRIP, and GISP2 ice cores across MIS 2 and palaeoclimatic implications. Quaternary Science Reviews 27, 18-28.

Shane, P.A.R., Smith, V.C., Lowe, D.J., Nairn, I.A., 2003. Re-identification of c. 15 700 cal BP tephra bed at Kaipo Bog, eastern North Island: implications for dispersal of Rotorua and Puketarata tephra beds. New Zealand Journal of Geology and Geophysics 46, 591-596.

Shane, P.A.R., Nairn, I.A., Martin, S.B., Smith, V.C., 2008. Compositional heterogeneity in tephra deposits resulting from the eruption of multiple magma bodies: implications for tephrochronology. Quaternary International 178, 44-53.

Turney, C.S.M., van den Burg, K., Wastegård, S., Davies, S.M., Whitehouse, N.J., Pilcher, J.R., Callaghan, C., 2006. North European last glacial–interglacial transition (LGIT; 15–9 ka) tephrochronology: extended limits and new events. Journal of Quaternary Science 21, 335-345.

Wohlfarth, B., Blaauw, M., Davies, S.M., Andersson, M., Wastegård, S., Hormes, A., Posnert, G., 2006. Constraining the age of Lateglacial and early Holocene pollen zones and tephra horizons in southern Sweden with Bayesian probability methods. Journal of Quaternary Science 21, 321-334.

Captions to figures and tables

Fig. 1. Study area in the vicinity of southern Japan showing locations of core site MD98-2195, Kuchierabujima and Tanegashima islands (including site T-1：30 ° 38'36.35"N, 130 ° 59'24.43"E), and various other volcanoes and calderas (C). Triangles represent volcanoes.

Fig. 2. Late Pleistocene and Holocene tephrostratigraphy in core MD98-2195 in the East China Sea, including depths of tephras A to C, and on the central part of Tanegashima Island (site T-1), including positions of tephras T-1-1 to T-1-3. K-Ah, Kikai-Akahoya tephra; AT, Aira-Tn tephra. White parts in the sections of the MD98-2195 and site T-1 denote grey silt and clay sediments, and tephric light-brown soils respectively.

Fig. 3. Defined members of (A) Sakurajima-Satsuma tephra and (B) Noike-Yumugi tephra on Tanegashima Island. pfa: pumice fall; afa: ash fall; bs: base surge deposit.

Fig. 4. Oxide variation diagrams of glass composition (wt%) showing correlation of Sakurajima-Satsuma (Sz-S) tephra (including samples from sites on Osumi and Satsuma peninsulas) with unknown late Pleistocene tephras on Tanegashima Island and at MD98-2195 in the East China Sea. The electron microprobe analyses for tephra

MD98-2195-A, analysed at TMU, were corrected using analyses of glass from Aira-Tn tephra (see text).

Fig. 5. Oxide variation diagrams of glass composition (wt%) showing correlation of Noike-Yumugi (N-Ym) tephra (upper, middle, and lower units) with unknown late Pleistocene tephras in Tanegashima Island and at MD98-2195 in the East China Sea. The electron microprobe analyses for tephra MD98-2195-B and -C analysed at TMU, were corrected using analyses of glass from Aira-Tn tephra (see text).

Fig. 6. Stratigraphic positions of (A) Sakurajima-Satsuma (Sz-S) and (B) Noike-Yumugi (N-Ym) tephras with respect to the marine oxygen isotope records in core MD98-2195. Also shown is position of tephra C (uncorrelated), aged c. 20,000 cal BP.
*1, Marine oxygen isotope curve and stratigraphic positions of AT and K-Ah are after Ijiri et al. (2005). Note that the ages of AT and K-Ah slightly differ from those described in the text, which are probably more suitable.

Fig. 7. Approximate distributions of Sakurajima-Satsuma (Sz-S) and Noike-Yumugi (N-Ym) tephras. N-Ym (u) denotes the upper unit and N-Ym (m, l) denotes the middle/lower units of N-Ym. Broken and dotted lines show the approximate extents of tephras Sz-S and N-Ym, respectively.

Table 1 Average major-element composition of glass shards from Aira-Tn (AT) tephra, used as an in-house standard for electron microprobe analysis.

Notes: Analyses undertaken on a Cameca SX-50 wavelength dispersive microprobe at University of Toronto, on a JXA-8600SX wavelength dispersive microprobe at Kagoshima University, and on a JEOL JED-2300 energy dispersive X-ray spectrometer at Tokyo Metropolitan University. Operating conditions are 15 kV accelerating voltage, 10 μm beam diameter and 10 nA beam current for University of Toronto and Kagoshima University, and 15 kV accelerating voltage, 10 μm beam diameter and 1.2 nA beam current for Tokyo Metropolitan University. Standardization achieved using mineral and glass standards. Analyses normalized to 100% on a water-free basis. H_2O_d = water by difference; total iron expressed as FeO_t; (#) = standard deviation; n = number of shards analysed.

Table 2 Average major-element composition (normalized) of glass shards from proximal N-Ym tephra on Kuchierabujima Island and from proximal Sz-S tephra on Osami and Satsuma peninsulas, southern Kyushu.

*1) After Moriwaki et al. (2009). Analysed at Kagoshima University for N-Ym and at the University of Toronto for Sz-S. See Table 1 for conditions of analysis.

Table 3 Average major-element composition (normalized) of glass shards from tephra A (correlated here with Sakurajima-Satsuma tephra, Sz-S), tephra B (correlated here with Noike-Yumugi tephra, N-Ym), and tephra C (uncorrelated) in core MD98-2195, and of glass shards from samples T-1-1 and T-1-2 of Noike-Yumugi tephra at site T-1 on Tanegashima Island.

Tephras MD98-2195-A, -B, -C were analysed at Tokyo Metropolitan University. Values for oxides of Ca, Na, and K are those obtained before corrections using AT glass compositions as an in-house standard (see text). Tephras from Tanegashima were analysed at Kagoshima University. See Table 1 for conditions of analysis.

Table 1

Tephra name	AT	AT	AT
Sample number	KU1 & KU35	UT1304 & UT1305	AT091224
Laboratory	Kagoshima Univ.	Univ. of Toronto	Tokyo Metropolitan Univ.
SiO_2	77.95 (0.25)	78.13 (0.22)	78.91 (0.39)
Al_2O_3	12.45 (0.15)	12.21 (0.14)	12.09 (0.11)
TiO_2	0.14 (0.07)	0.13 (0.03)	0.14 (0.05)
FeO_t	1.24 (0.05)	1.26 (0.05)	1.28 (0.11)
MnO	0.03 (0.02)	0.05 (0.03)	0.08 (0.04)
MgO	0.11 (0.05)	0.12 (0.01)	0.11 (0.04)
CaO	1.15 (0.05)	1.16 (0.05)	0.72 (0.06)
Na_2O	3.51 (0.17)	3.62 (0.11)	3.03 (0.35)
K_2O	3.43 (0.18)	3.33 (0.07)	3.66 (0.10)
H_2O_d	3.43 (0.79)	5.34 (0.29)	6.34 (1.52)
n	15	30	12

Notes: Analyses undertaken on a Cameca SX-50 wavelength dispersive micro-probe at University of Toronto, on JXA-8600SX at Kagoshima University and on JEOL JED-2300 energy dispersive X-ray spectrometer at Tokyo Metropolitan Univeristy. Operating conditions are 15 kV accelerating voltage, 10 µm beam diameter and 10 nA beam current for University of Toronto and Kagoshima Univeristy, and 15 kV accelerating voltage, 10 µm beam diameter and 1.2 nA beam current for Tokyo Metropolitan Univerisity. Standardization achieved using mineral and glass standards. Analyses recast to 100% on a water-free basis. H_2O_d = water by difference, total iron oxide as FeOt, (#) = standard deviation, and n = number of shards analysed.

鹿児島大学KU，トロント大UT，首都大のAT化学組成

鹿児島大　KU1：　AT(Ito pfl) 加治木町鶴原：チェック用試料

	SiO2	Al2O3	TiO2	FeO	MnO	MgO	CaO	Na20	K2O	water	sum
	77.88	12.48	0.17	1.27	0	0.14	1.16	3.56	3.33	2.82	100
	77.8	12.63	0.08	1.28	0.03	0.08	1.17	3.58	3.34	3.64	100
	78.28	12.28	0.08	1.17	0.02	0.15	1.23	3.387	3.41	3.74	100
	78.09	12.34	0.18	1.15	0.02	0.12	1.18	3.443	3.47	3.56	100
	78.43	12.12	0.19	1.25	0	0.11	1.21	3.513	3.18	2.92	100
aver	78.1	12.37	0.14	1.22	0.01	0.12	1.19	3.497	3.35	3.336	100
stdev	0.264	0.193	0.05	0.06	0.01	0.03	0.03	0.081	0.11	0.4316017	

一般的なAT glassの組成とよく合っているので，測定条件に問題はない．

KU35　AT チェック

	SiO2	Al2O3	TiO2	FeO	MnO	MgO	CaO	Na20	K2O	water	
	78.03	12.49	0.1	1.29	0.05	0.17	1.16	3.356	3.36	4.05	100
	77.84	12.57	0.13	1.21	0.03	0.04	1.12	3.794	3.26	1.68	100
	77.79	12.65	0.26	1.25	0.02	0.01	1	2.918	4.1	2.68	100
	78.11	12.38	0	1.34	0.06	0.15	1.26	3.366	3.33	3.16	100
	77.41	12.48	0.19	1.3	0.06	0.16	1.13	3.635	3.63	2.35	100
	77.87	12.48	0.11	1.21	0.02	0.08	1.15	3.648	3.42	3.78	100
	77.84	12.49	0.22	1.18	0.02	0.01	1.13	3.483	3.64	3.25	100
	77.95	12.64	0	1.23	0	0.06	1.1	3.612	3.4	3.93	100
	77.77	12.37	0.22	1.25	0.06	0.17	0.99	3.622	3.54	5.03	100
	77.39	12.68	0.17	1.3	0.08	0.07	1.12	3.774	3.4	5.4	100
aver	77.8	12.52	0.14	1.26	0.04	0.09	1.12	3.521	3.51	3.531	100
stdev	0.236	0.109	0.09	0.05	0.03	0.06	0.08	0.259	0.24	1.1543392	

トロント大：UT　AT-Tephra Formation :UT1305(88032201-3, Iwato, Kagoshima) Aira caldera

No.	SiO2	Al2O3	TiO2	FeO	MnO	MgO	CaO	Na20	K2O	Na2O+K2O	Cl2O
1	78.44	11.74	0.12	1.24	0.06	0.12	1.22	3.572	3.38	6.9546891	0.105374
2	78.09	12.21	0.06	1.19	0.02	0.13	1.2	3.757	3.22	6.9767442	0.126276
3	77.63	12.4	0.13	1.33	0.04	0.12	1.1	3.782	3.38	7.1639275	0.094817
4	78.26	12.06	0.14	1.3	0.03	0.12	1.25	3.359	3.35	6.7068019	0.137305
5	77.91	12.45	0.08	1.23	0.02	0.13	1.16	3.476	3.43	6.9103973	0.11623
6	77.64	12.42	0.09	1.29	0.11	0.12	1.16	3.68	3.34	7.0241851	0.147213
7	78.16	12.17	0.14	1.2	0.05	0.13	1.15	3.516	3.38	6.8932554	0.106213
8	78.14	12.13	0.16	1.14	0.04	0.1	1.09	3.783	3.3	7.0802071	0.12681
9	78.15	12.13	0.18	1.24	0.03	0.11	1.05	3.658	3.33	6.9880537	0.137435
10	78.2	12.05	0.13	1.34	0	0.12	1.12	3.554	3.41	6.9594738	0.084872
11	78.05	12.3	0.12	1.25	0.1	0.14	1.13	3.484	3.34	6.8208215	0.105585
12	77.85	12.33	0.16	1.21	0.05	0.16	1.14	3.636	3.36	6.995972	0.106
13	78.42	11.95	0.06	1.32	0.02	0.13	1.19	3.554	3.17	6.7255507	0.180909
14	77.6	12.41	0.12	1.23	0.06	0.12	1.15	3.798	3.4	7.1956109	0.116058
15	77.98	12.17	0.14	1.28	0.1	0.12	1.2	3.623	3.26	6.8863227	0.127132
aver.	78.03	12.19	0.12	1.25	0.05	0.12	1.15	3.616	3.34	6.9521342	0.121215
stdev	0.266	0.197	0.03	0.06	0.03	0.01	0.05	0.13	0.07		0.023716

UT　AT (Ito formation) :UT1304

Locality: Iwato, Kokubu, Field no. 88032201(2)　n:15

No.	SiO2	Al2O3	TiO2	FeO	MnO	MgO	CaO	Na20	K2O	Na2O+K2O	Cl2O
1	78.33	12.12	0.16	1.21	0.02	0.14	1.14	3.536	3.24	6.7768073	0.10523
2	77.96	12.3	0.11	1.22	0.04	0.12	1.18	3.636	3.37	7.0099842	0.073568
3	77.98	12.16	0.13	1.34	0.05	0.12	1.17	3.73	3.21	6.9434201	0.115899
4	77.64	12.31	0.15	1.33	0.07	0.14	1.17	3.684	3.39	7.07463	0.115461
5	78.11	12.29	0.11	1.27	0.01	0.13	1.15	3.56	3.25	6.8121623	0.116538
6	77.86	12.25	0.15	1.24	0.06	0.12	1.16	3.759	3.28	7.035598	0.126011
7	78.25	12.12	0.11	1.23	0.05	0.09	1.16	3.582	3.3	6.8787528	0.105341
8	78.24	12.12	0.12	1.34	0.07	0.12	1.17	3.443	3.3	6.7389702	0.094767
9	78.06	12.09	0.14	1.23	0.07	0.12	1.18	3.654	3.34	6.992126	0.125984
10	77.97	12.21	0.08	1.24	0.01	0.14	1.26	3.591	3.35	6.9397641	0.14743
11	77.78	12.33	0.1	1.3	0.08	0.14	1.15	3.582	3.38	6.9639649	0.158512
12	78.24	12.19	0.17	1.19	0	0.12	1.15	3.555	3.26	6.8145967	0.136713
13	78.17	12.12	0.16	1.3	0.07	0.11	1.06	3.581	3.36	6.9406296	0.073949
14	77.95	12.22	0.15	1.18	0.06	0.14	1.13	3.706	3.39	7.0962308	0.0737
15	78.06	12.04	0.16	1.25	0.05	0.13	1.14	3.601	3.4	7.001474	0.168457
aver.	78.04	12.19	0.13	1.26	0.05	0.12	1.16	3.613	3.32	6.9346074	0.115837
stdev	0.191	0.09	0.03	0.05	0.03	0.01	0.04	0.083	0.06		0.029537

首都大学東京：鈴木研究室EDSによるAT測定 /

AT チェック：0912首都大学東京EDS, 分析者：鈴木，村田

	SiO2	Al2O3	TiO2	FeO	MnO	MgO	CaO	Na2O	K2O	Water	
1	78.62	12.1	0.03	1.38	0.07	0.13	0.74	3.32	3.62	7.17	92.83
2	78.5	12.05	0.17	1.26	0.09	0.15	0.8	3.37	3.61	5.02	94.98
3	78.82	12.29	0.12	1.2	0.12	0.06	0.71	3.05	3.63	5.92	94.08
4	78.86	11.93	0.14	1.23	0.08	0.14	0.81	3.18	3.63	3.84	96.16
5	78.3	12.27	0.19	1.32	0.11	0.07	0.67	3.17	3.89	4.91	95.09
6	78.98	11.95	0.1	1.21	0.05	0.14	0.68	3.17	3.73	7.34	92.66
7	79.15	12.14	0.21	1.43		0.04	0.67	2.78	3.6	7.98	92.02
8	79.13	12	0.17	1.24	0.04	0.14	0.67	3	3.61	7.82	92.18
9	78.88	12.1	0.11	1.16	0.11	0.07	0.69	3.21	3.67	4.16	95.84
10	78.7	12.04	0.13	1.49	0.14	0.12	0.68	3.02	3.68	6.69	93.31
11	79.14	12.08	0.18	1.21	0.02	0.13	0.71	3.05	3.47	7.1	92.9
12	79.83	12.1	0.07	1.25		0.17	0.82	2.02	3.75	8.11	91.89
aver.	78.91	12.09	0.14	1.28	0.08	0.11	0.72	3.028	3.66	6.34	93.66
stdev	0.39	0.11	0.05	0.11	0.04	0.04	0.06	0.35	0.1	1.52	

成の比較

鹿児島大学でのAT分析値（KU1とKU35の平均）

Na2O+K2O	SiO2	Al2O3	TiO2	FeO	MnO	MgO
6.894423	77.94799	12.44703	0.140752	1.239574	0.028054	0.107769
6.921959	0.250309	0.151032	0.070787	0.054228	0.020293	0.045237
6.794099						
6.916217						
6.695509						
6.844442						

Na2O+K2O
6.711829
7.058584
7.018085
6.69145
7.260625
7.067138
7.121447
7.015718
7.160156
7.17759
7.028262

UT1305:　Cl2Oを除いた値

water	Water+Cl2O		SiO2	Al2O3	TiO2	FeO	MnO	MgO
5.1	5.205374		78.52291	11.75101	0.116033	1.244721	0.063291	0.116033
4.97	5.096276		78.19043	12.22219	0.063218	1.19061	0.021073	0.126436
5.08	5.174817		77.70762	12.41171	0.126542	1.328696	0.042181	0.115997
5.32	5.457305		78.37099	12.07823	0.137493	1.300895	0.031729	0.11634
5.36	5.47623		77.99622	12.46162	0.084629	1.227121	0.021157	0.126944
4.9	5.047213		77.75889	12.43679	0.094777	1.295279	0.105307	0.115838
5.85	5.956213		78.24545	12.18498	0.138224	1.201486	0.053163	0.127591
5.37	5.49681		78.23526	12.14689	0.158714	1.142738	0.042324	0.095228
5.41	5.547435		78.25501	12.14265	0.17997	1.238614	0.031759	0.105864
5.74	5.824872		78.26512	12.06202	0.127416	1.337865	0	0.116798
5.29	5.395585		78.1316	12.31376	0.116267	1.247231	0.095128	0.137407
5.66	5.766		77.92869	12.34083	0.159168	1.209677	0.053056	0.159168
6.03	6.210909		78.56084	11.97229	0.063966	1.321963	0.021322	0.127932
5.22	5.336058		77.69088	12.42209	0.116193	1.235871	0.063378	0.116193
5.61	5.737132		78.08412	12.18838	0.137902	1.283546	0.09547	0.116686
5.394	5.51	aver.	78.1296	12.20903	0.121367	1.253754	0.049356	0.121364
0.328085	0.332261	stdev	0.271175	0.19721	0.033757	0.056408	0.030833	0.014469

AT (Ito formation) :UT1304　：Cl2Oを除いた値

Water	Water+Cl2O		SiO2	Al2O3	TiO2	FeO	MnO	MgO
4.97	5.07523		78.41549	12.13523	0.158011	1.211416	0.021068	0.136943
4.85	4.923568		78.01885	12.30548	0.105175	1.220031	0.04207	0.115693
5.09	5.205899		78.0697	12.17301	0.126582	1.339664	0.052743	0.116034
4.73	4.845461		77.73188	12.32655	0.14712	1.334588	0.07356	0.136611
5.61	5.726538		78.20359	12.30383	0.106068	1.27281	0.010607	0.127281
4.77	4.896011		77.96235	12.27	0.147198	1.240669	0.063085	0.115656
5.07	5.175341		78.32938	12.13747	0.105452	1.233783	0.052726	0.094906
5.03	5.124767		78.30963	12.13114	0.115936	1.338536	0.073778	0.115936
4.75	4.875984		78.15622	12.10975	0.136655	1.229896	0.073584	0.115631
5.04	5.18743		78.08446	12.22311	0.08437	1.244458	0.010546	0.137101
5.37	5.528512		77.90047	12.35188	0.095259	1.301869	0.084674	0.137596
4.91	5.046713		78.349	12.20517	0.168492	1.189978	0	0.115839
5.34	5.413949		78.23241	12.12602	0.158579	1.30035	0.074004	0.105719
5.02	5.0937		78.01098	12.23268	0.147509	1.180069	0.063218	0.136972
5.02	5.188457		78.1899	12.06491	0.158194	1.255004	0.052731	0.126555
5.038		Average	78.13095	12.20642	0.130707	1.259541	0.049893	0.122298
0.244809		Stdev	0.176815	0.090688	0.026749	0.053076	0.026949	0.012949

UT1304とUT1305の平均 (測定個数n. 30):最終版

	SiO2	Al2O3	TiO2	FeO	MnO	MgO
Average	78.13028	12.20772	0.126037	1.256648	0.049624	0.121831
Stdev	0.223995	0.143949	0.030253	0.054742	0.028891	0.013709

AT091224: TMU　Suzuki Lab. (測定個数：n.12)

	SiO2	Al2O3	TiO2	FeO	MnO	MgO
Aver.	78.90917	12.0875	0.135	1.281667	0.083	0.113333
Stdev	0.39	0.11	0.05	0.11	0.04	0.04

測定個数n:15

CaO	Na20	K2O	water	sum
1.152486	3.508686	3.427666	3.4335	100
0.05164	0.169884	0.175102	0.79297	

CaO	Na20	K2O	Water	Sum
1.223624	3.575936	3.386063	5.21	100
1.201147	3.761485	3.22413	5.1	100
1.096701	3.785729	3.385011	5.17	100
1.248013	3.36329	3.352713	5.46	100
1.163649	3.480369	3.438054	5.48	100
1.15838	3.685755	3.348771	5.05	100
1.148323	3.519397	3.381173	5.96	100
1.089834	3.787966	3.301244	5.5	100
1.048058	3.66291	3.33473	5.55	100
1.125506	3.557023	3.408371	5.82	100
1.130963	3.488018	3.340041	5.4	100
1.14601	3.639643	3.363752	5.77	100
1.194031	3.560771	3.176975	6.21	100
1.151367	3.802681	3.401287	5.34	100
1.198683	3.627873	3.267207	5.74	100
1.154953	3.619923	3.340635	5.517333	100
0.053235	0.130394	0.071473	0.331629	

CaO	Na20	K2O	Water	
1.137678	3.539442	3.244488	5.08	100
1.17796	3.639057	3.376119	4.92	100
1.170887	3.734181	3.217303	5.21	100
1.166451	3.688508	3.394268	4.85	100
1.156136	3.563869	3.256273	5.73	100
1.156555	3.764062	3.280412	4.9	100
1.159967	3.585351	3.300632	5.18	100
1.169902	3.446467	3.298912	5.12	100
1.177336	3.658153	3.342795	4.88	100
1.26555	3.596272	3.353708	5.19	100
1.153689	3.588078	3.386977	5.53	100
1.147855	3.559404	3.264542	5.05	100
1.057195	3.58389	3.361879	5.41	100
1.127387	3.708788	3.392698	5.09	100
1.138995	3.606818	3.406439	5.19	100
1.15757	3.617489	3.325163	5.155333	100
0.043231	0.082858	0.060585	0.255297	

CaO	Na20	K2O	Water	
1.156261	3.618706	3.332899	5.336333	100
0.048233	0.106626	0.066029	0.293463	

CaO	Na2O	K2O	Water
0.720833	3.028333	3.6575	6.34
0.06	0.35	0.1	1.52

Tephra name	N-Ym			Sz-S	
Location	Kuchierabujima[*1)]			Osumi Peninsula	Satsuma Peninsula
Stratigraphy	Upper	Middle	Lower		
Reference No.	KU5	KU4	KU2		
SiO_2	77.37 (1.84)	73.29 (0.87)	74.90 (0.42)	74.58 (0.23)	74.58 (0.48)
Al_2O_3	12.43 (0.47)	13.27 (0.48)	12.94 (0.17)	13.53 (0.16)	13.48 (0.35)
TiO_2	0.34 (0.17)	0.61 (0.09)	0.49 (0.09)	0.34 (0.07)	0.39 (0.09)
FeO_t	1.42 (0.61)	3.27 (0.33)	2.47 (0.18)	1.93 (0.09)	1.94 (0.11)
MnO	0.06 (0.06)	0.10 (0.04)	0.06 (0.05)	0.07 (0.03)	0.05 (0.03)
MgO	0.31 (0.24)	0.64 (0.16)	0.48 (0.05)	0.42 (0.03)	0.52 (0.16)
CaO	1.49 (0.67)	2.72 (0.43)	2.14 (0.11)	2.18 (0.12)	2.15 (0.24)
Na_2O	3.67 (0.12)	3.38 (0.18)	3.61 (0.17)	3.96 (0.15)	3.96 (0.12)
K_2O	2.91 (0.19)	2.71 (0.19)	2.88 (0.06)	2.99 (0.11)	2.93 (0.13)
H_2O_d	4.50 (1.90)	8.26 (3.67)	5.72 (1.38)	4.55 (1.22)	6.56 (1.83)
n	9	11	10	47	29

*1) After Moriwaki et al.(2009), Analysed at Kagoshima University for N-Ym and at University of Toronto for Sz-S. See Table 1 for the conditions of analysis

Table 3

Location	MD982195			Tanegashima	
Sample name	A	B	C	T-1-1	T-1-2
Sample depth	9.120-9.128 m	9.30-9.33 m	15.25-15.30 m	68 cm	98 cm
Reference No.	No.142-1	No.142-2	No.142-3	KU12	KU13
SiO_2	75.51 (0.18)	75.47 (1.95)	77.92 (1.61)	75.31 (1.04)	74.41 (1.35)
Al_2O_3	13.20 (0.13)	12.82 (0.48)	12.32 (0.69)	13.58 (0.36)	13.05 (0.20)
TiO_2	0.43 (0.06)	0.53 (0.18)	0.20 (0.13)	0.34 (0.13)	0.54 (0.12)
FeOt	1.93 (0.09)	2.38 (0.69)	1.40 (0.27)	1.79 (0.10)	2.81 (0.69)
MnO	0.08 (0.04)	0.09 (0.06)	0.08 (0.05)	0.07 (0.04)	0.07 (0.04)
MgO	0.38 (0.06)	0.40 (0.18)	0.15 (0.10)	0.40 (0.12)	0.57 (0.17)
CaO	1.74 (0.09)	1.76 (0.60)	0.95 (0.52)	2.02 (0.32)	2.39 (0.34)
Na_2O	3.42 (0.15)	3.35 (0.33)	3.36 (0.54)	3.52 (0.44)	3.27 (0.49)
K_2O	3.32 (0.08)	3.20 (0.35)	3.62 (0.38)	2.97 (0.11)	2.89 (0.13)
H_2O_d	4.16 (1.03)	5.31 (2.41)	5.24 (2.15)	3.62 (1.28)	1.59 (0.84)
n	16	16	20	10	10

Figure 1

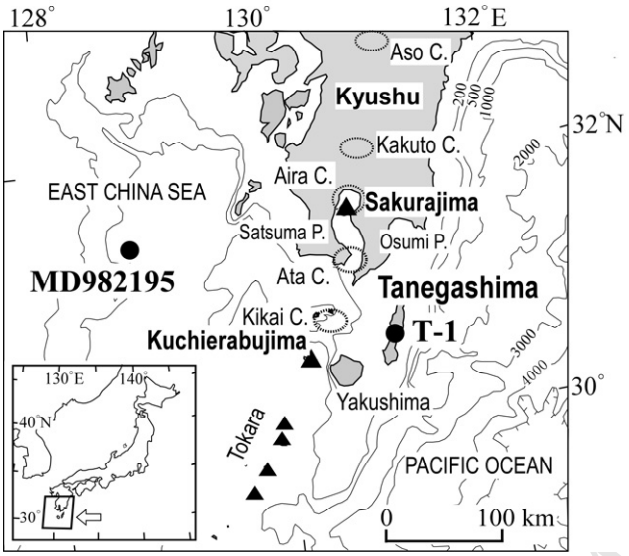

Figure 2

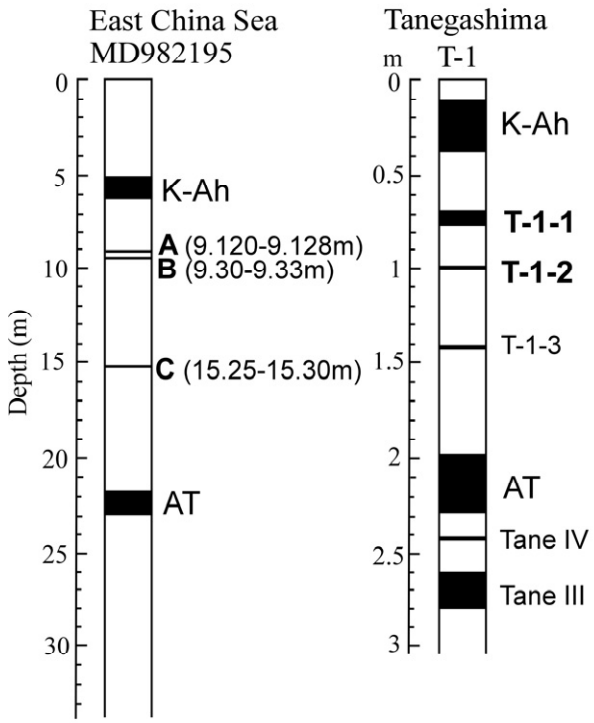

Figure 3

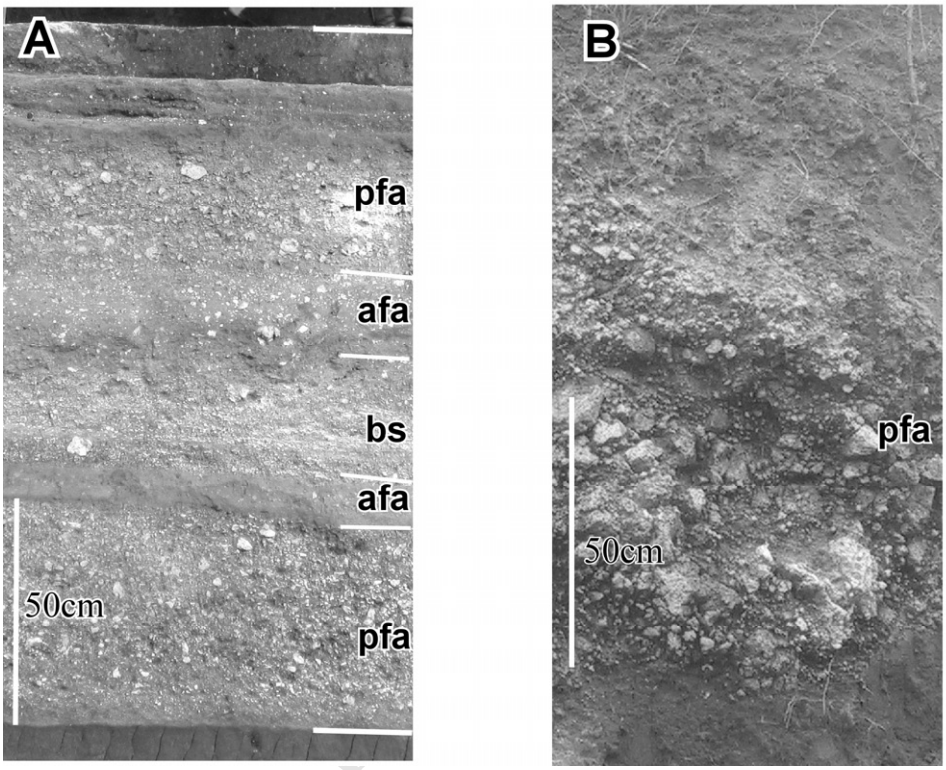

Figure 4

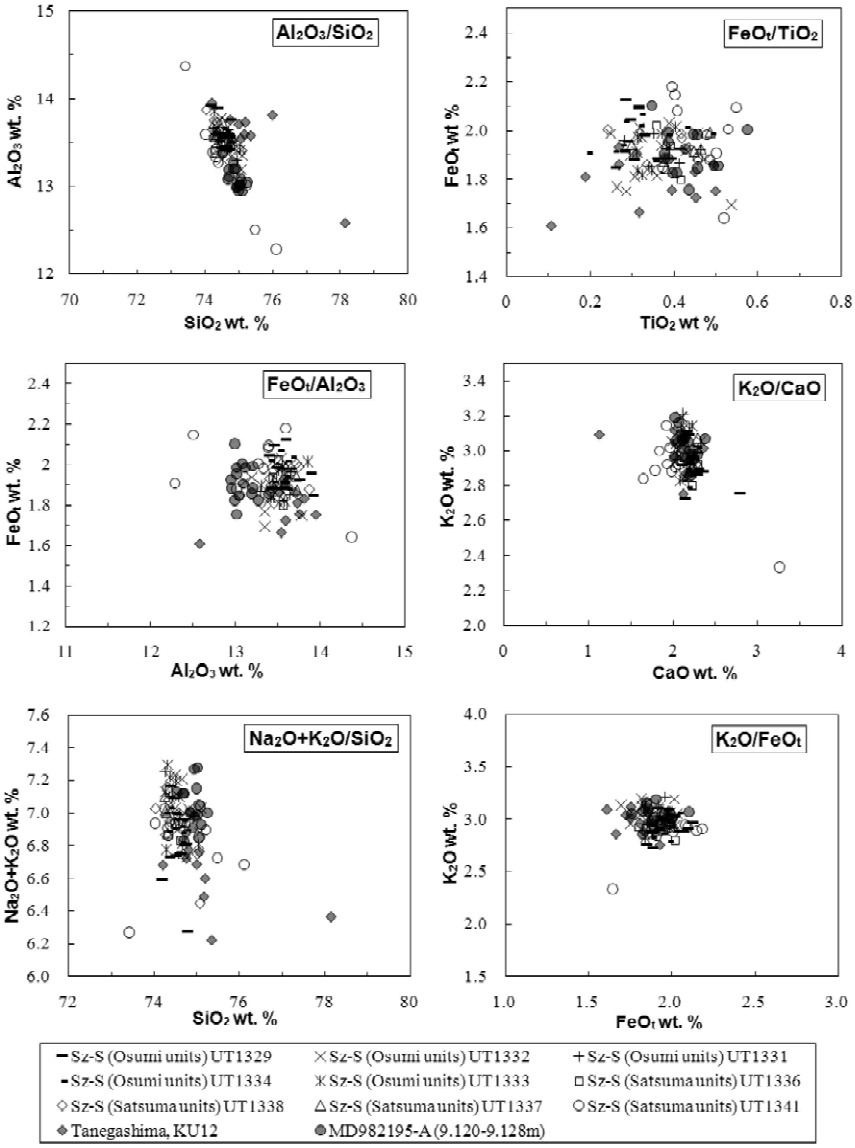
Al2O3/SiO2
Al2O3 wt. %
SiO2 wt. %
FeOt/TiO2
FeOt wt %
TiO2 wt %
FeOt/Al2O3
FeOt wt. %
Al2O3 wt. %
K2O/CaO
K2O wt. %
CaO wt. %
Na2O+K2O/SiO2
Na2O+K2O wt. %
SiO2 wt. %
K2O/FeOt
K2O wt. %
FeOt wt. %
Sz-S (Osumi units) UT1329
Sz-S (Osumi units) UT1332
Sz-S (Osumi units) UT1331
Sz-S (Osumi units) UT1334
Sz-S (Osumi units) UT1333
Sz-S (Satsuma units) UT1336
Sz-S (Satsuma units) UT1338
Sz-S (Satsuma units) UT1337
Sz-S (Satsuma units) UT1341
Tanegashima, KU12
MD982195-A (9.120-9.128m)

Figure 5

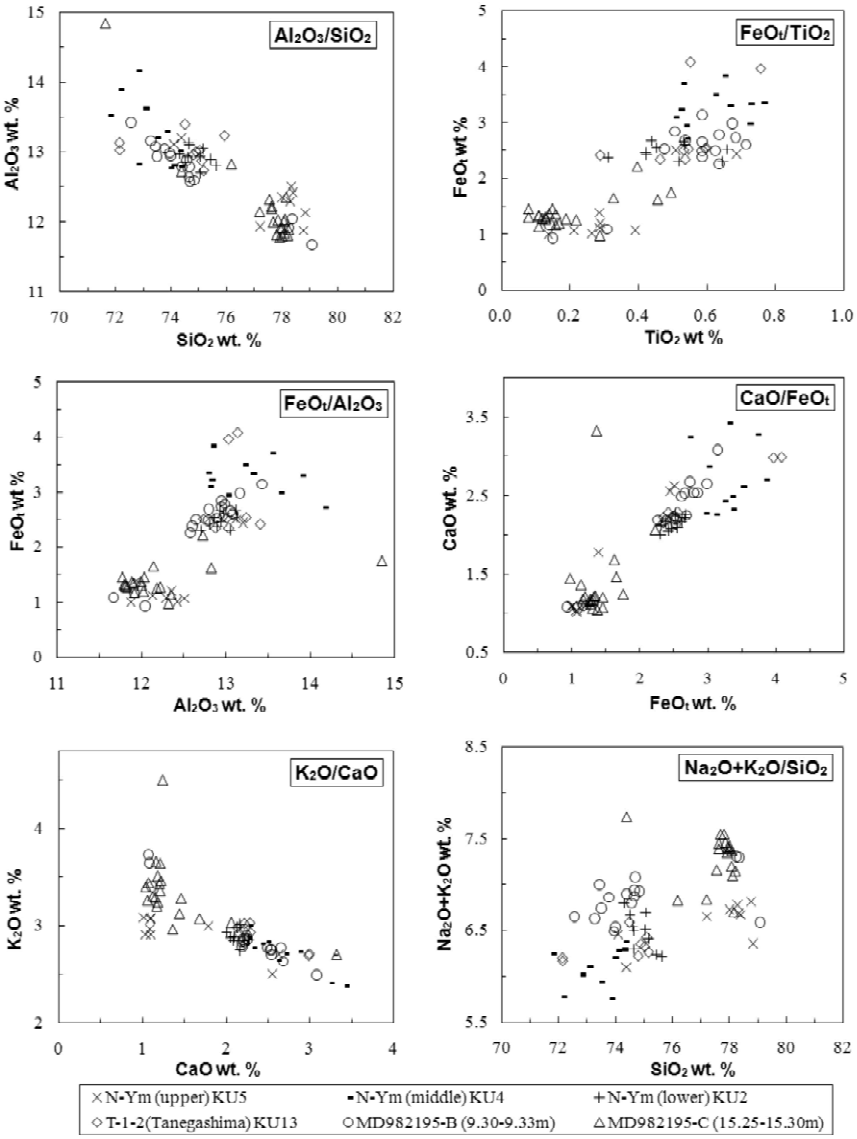
Al2O3/SiO2
Al2O3 wt. %
SiO2 wt. %
FeOt/TiO2
FeOt wt %
TiO2 wt %
FeOt/Al2O3
FeOt wt %
Al2O3 wt. %
CaO/FeOt
CaO wt. %
FeOt wt. %
K2O/CaO
K2O wt. %
CaO wt. %
Na2O+K2O/SiO2
Na2O+K2O wt. %
SiO2 wt. %
×N-Ym (upper) KU5
▪N-Ym (middle) KU4
+N-Ym (lower) KU2
◇T-1-2(Tanegashima) KU13
○MD982195-B (9.30-9.33m)
△MD982195-C (15.25-15.30m)

Figure 6

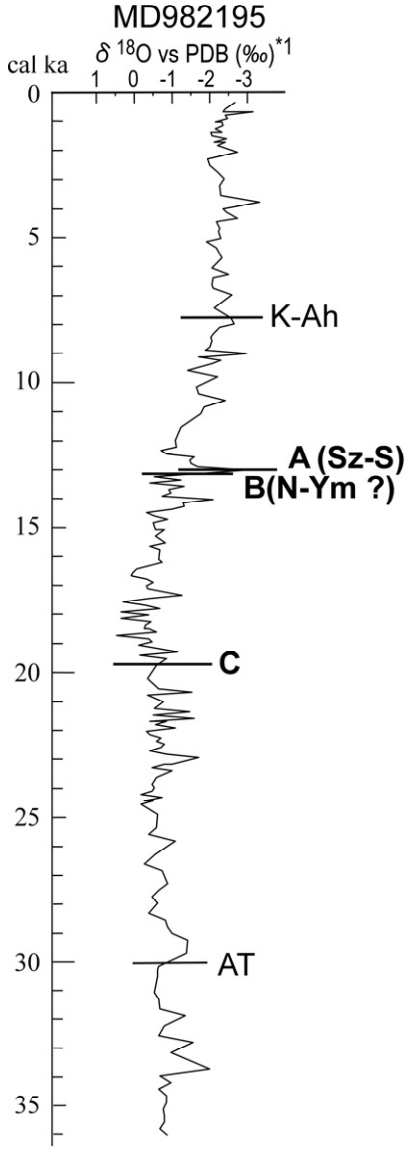
MD982195
cal ka
δ 18O vs PDB (‰)*1
1 0 -1 -2 -3
0
5
10
15
20
25
30
35
K-Ah
A (Sz-S)
B(N-Ym ?)
C
AT

Figure 7